# Airborne determination of the temporo-spatial distribution of benzene, toluene, nitrogen oxides and ozone in the boundary layer across Greater London, UK

**M.D Shaw[1], J.D Lee[2], B. Davison[1], A.Vaughan[3], R.M Purvis[2], A. Harvey[3], A.C. Lewis[2], C. N. Hewitt[1]**

[1] {Lancaster Environment Centre, Lancaster University, Lancaster, UK}
[2] {National Centre for Atmospheric Science, University of York, York, UK}
[3] {Department of Chemistry, University of York, York, UK}
Correspondence to: C.N. Hewitt (n.hewitt@lancaster.ac.uk)

## Keywords

Airborne measurements, volatile organic compounds, benzene, toluene, nitrogen oxides, ozone, proton transfer reaction mass spectrometer, chemiluminescence detector, Automatic Hydrocarbon Network, Automatic Urban Rural Network, air quality, pollution, London.

## Abstract

Highly spatially resolved mixing ratios of benzene and toluene, nitrogen oxides ($NO_x$) and ozone ($O_3$) were measured in the atmospheric boundary layer above Greater London during the period 24th June to 9th July 2013 using a Dornier 228 aircraft. Toluene and benzene were determined in-situ using a proton transfer reaction mass spectrometer (PTR-MS), $NO_x$ by dual channel NO*x* chemiluminescence and $O_3$ mixing ratios by UV absorption.

Average mixing ratios observed over inner London at 360±10 m a.g.l. were 0.20±0.05, 0.28±0.07, 13.2±8.6, 21.0±7.3 and 34.3±15.2 ppbv for benzene, toluene, NO, $NO_2$ and $NO_x$ respectively. Linear regression analysis between $NO_2$, benzene and toluene mixing ratios yield a strong covariance indicating that these compounds predominantly share the same or co-located sources within the city.

Average mixing ratios measured at 360±10 m a.g.l. over outer London were always lower than over inner London. Where traffic densities were highest, the toluene/benzene (T/B)

concentration ratios were highest (average of 1.8 ± 0.5 ppbv ppbv$^{-1}$) indicative of strong local sources. Daytime maxima in $NO_x$, benzene and toluene mixing ratios were observed in the morning (~ 40 ppbv $NO_x$, ~350 pptv toluene and ~200 pptv benzene) and for ozone in the mid-afternoon (~ 40 ppbv $O_3$) all at 360±10 m a.g.l.

## 1 Introduction

Ground level ozone ($O_3$) is a secondary pollutant, produced from photochemical reactions involving volatile organic compounds (VOCs) and nitrogen oxides ($NO_x$ = NO + $NO_2$). Ozone has significant detrimental effects on human health and vegetation while $NO_2$ and some VOCs also have, themselves, direct effects on health. Whilst the basic atmospheric chemistry leading to $O_3$ formation is generally well understood, there are substantial uncertainties associated with the magnitude and speciation of emissions of both VOCs and $NO_x$ from urban areas, leading to uncertainties in the detailed understanding of urban photochemistry and air pollution.

In urban areas the dominant anthropogenic sources of VOCs are vehicular exhaust, fuel evaporation and emissions from the commercial and industrial use of solvents (Karl et al., 2009;Langford et al., 2010). Vehicular emissions are the predominant source of VOCs to the atmosphere in urban and suburban areas, accounting for > 50% of the total (Watson et al., 2001;Na et al., 2005;Kansal, 2009) with a wide range of VOCs emitted directly due to fuel evaporation and from vehicular exhaust as unburnt fuel and as partially oxidized fuel components. The dominant urban sources of $NO_x$ are combustion processes, including vehicles. In the UK as a whole, about 50% of $NO_x$ is thought to be derived from vehicles, although this percentage is larger in urban areas (Lee et al., 2015).

VOC and $NO_x$ emissions from airports are also of importance, originating due to a combination of emissions from aircraft exhaust, ground support equipment (GSE) exhaust and evaporative losses during aircraft refuelling (Carslaw et al., 2006). High mixing ratios of aromatic compounds, such as toluene and benzene, and low $NO_x$ mixing ratios have been previously observed in jet engine exhaust immediately after ignition, attributed to low engine temperature causing incomplete combustion (Schürmann et al., 2007). Previous aircraft exhaust studies have shown toluene/benzene (T/B) ratios observed during engine ignition are up to 3.1 ppbv ppbv$^{-1}$, typical of kerosene fuel. At higher engine temperatures, i.e. during

taxiing, higher aromatics tend to crack leading to a reduced amount of these species, but increasing amounts of benzene. Thus for aircraft taxiing, a T/B ratio of ~0.5 ppbv ppbv$^{-1}$ was previously observed (Spicer et al., 1994). Similarly higher $NO_x$ mixing ratios are observed due to higher engine combustion. As well as the contribution from aircraft, additional emissions from airport environments occur during the handling of aircraft with GSE. The GSE vehicles are mostly diesel powered, leading to relatively high emission rates of the oxides of nitrogen. During aircraft refuelling, gaseous air-fuel mixtures are released from the aircraft tanks through fuel vents which can be discriminated by the observed T/B ratio, since kerosene fuel tends to have an enhanced amount of aromatic compounds. VOC emissions during engine refuelling were previously found to account for 2.7% of the total VOC emissions of Zurich airport (Schürmann et al., 2007).

Background and peak UK VOCs, $O_3$ and $NO_2$ mixing ratios are determined hourly by the national monitoring networks such as the Automatic Hydrocarbon Network (AHN) and the Automatic Urban and Rural Network (AURN), both operated by the Department of Environment, Food and Rural Affairs). Hourly mixing ratios of $NO_x$ species are currently measured at 130 network sites with selected VOCs measured at 4 sites. Within Greater London these sites form part of the London Air Quality Network (LAQN). However, measurements from these networks suffer from the limitations of being made at relatively few sites and so may not be representative of mixing ratios over larger spatial scales.

The development of fast-response analytical instruments for $NO_x$ and VOCs means that the mixing ratios of these analytes can now be measured at high spatial resolution from low-flying aircraft. The advantages of in-situ aircraft measurements are that they provide information on the horizontal and vertical distributions of air pollutants over a large spatial area allowing continuous gradients of mixing ratios to be observed across cities and their surrounding rural areas.

In this study, we investigate the mixing ratios of $O_3$, benzene, toluene, NO, $NO_2$ and $NO_x$ across the Greater London region during several flights using the Natural Environment Research Council (NERC) Atmospheric Research and Survey Facility Dornier 228 aircraft between 24$^{th}$ June and 9$^{th}$ July 2013. The aim of this work was to (i) quantitatively determine the vertical, horizontal spatial and temporal distribution of VOCs, $NO_x$ and ozone mixing

ratios across London from an airborne platform, with a view to identify dominant emission sources in the region using measured T/B concentration ratios and (ii) wherever possible, compare these fast response airborne measurements with hourly ground-level measurements made by the national monitoring networks.

## 2 Method

### 2.1 NERC Dornier 228

The NERC Dornier 228 is a twin-engine turbo-prop powered, non-pressurised aircraft operated by the Airborne Research and Survey Facility (ARSF) based at Gloucester airport in central England. The aircraft has a cabin volume of 14 $m^3$ and operated with a crew of 2 pilots and 4 scientists for the duration of the flights. The aircraft has a minimum and maximum airspeed of 65 and 95 m/s respectively producing a maximum range of 2400 km. The aircraft has a maximum payload of 5970 kg including fuel, with a maximum operational altitude for science of 4500 m.

### 2.2 Flight description

Six research flights (RF) totalling 15 hours in duration were conducted between the hours of 8:30 – 17:20 UTC (table 1). Figure 1a shows all flight legs conducted during the project, overlaid on a transport map of SE England. Here we will focus on data obtained in transects across London. Figure 1b shows a map of Greater London on which typical repeated south-westerly to north-easterly flight legs of ~50 km are plotted. Identical flight legs across Greater London were chosen due to tight air traffic regulations and to allow data analysis in both a temporal and spatial domain. The grey area represents the Greater London boundary, the black area the inner London boundary and the blue area London's congestion charging zone (CCZ) in which road traffic is heavily regulated and subject to financial charging. Airspeed and altitude were fixed during the flights across Greater London with mean values of 73±3 m $s^{-1}$ and 360±10 m a.g.l respectively (table 1).

A north-westerly wind direction was observed during the flights, perpendicular to the flight transects. (table 1). Perpendicular wind directions are useful in providing a cross section of pollutant mixing ratios across London. RF 1 focussed on vertically profiling the PBL above London. Boundary layer (BL) height determinations were made from a combination of airborne observations and ground based measurements. Approximately hourly lower cloud base altitude determinations were made from Heathrow airport using laser cloud based

recorder (LCBR) observations. The lowest observed cloud base was interpreted as BL height. Where cloud based observations were not available (during clear skies), temporally interpolated BL height determinations from aircraft observations were used. Briefly, before commencing the city transects, a spiral descent from 2500 to 350 m a.g.l was performed 70 km south of London (position BL 1, figure 1b). Similarly, immediately after completing the city transects, a spiral ascent from 350 to 2500 m was performed directly north of London (position BL 2, figure 1b). These manoeuvres were performed to determine the height of the BL before and after the flights.

## 2.3 Meteorological and GPS sampling

Core equipment on the aircraft consisted of an Aircraft Integrated Meteorological Measurement System (AIMMS-20) turbulence probe (Aventech Research Inc.) mounted in an underwing PMS type pylon. The instrument is capable of precisely defining the aircraft altitude and velocity to within fractions of one metre per second with a temperature and humidity measurement precision of approximately 1%. This information is combined with fully compensated air-data measurements to compute wind speed with an accuracy of 0.5 knot and wind direction accuracy of 5 – 10 degrees (Beswick et al., 2008). The 3D position of the aircraft was measured using an IPAS 20 (Leica) inertial position and altitude system at an accuracy of 0.05 – 0.3 metres. All variables were acquired at a data acquisition rate of 20 Hz.

## 2.4 $NO_x$ sampling

$NO_x$ was measured from the aircraft using a fast time resolution (10Hz), high sensitivity $NO_x$ chemiluminescence system built by Air Quality Design, Inc. The instrument has a dual channel architecture for independent quantification of NO and $NO_2$. Each channel has a sample flow of 1.5 L $min^{-1}$ to ensure the required fast response time. Both sample flows are continually humidified to ensure that any changes in ambient humidity do not change the instrument sensitivity due to quenching of the chemiluminescence by water vapour. A detailed review of a similar system was described by (Lee et al., 2009), being a single channel instrument which operates using the same principles at the Cape Verde Atmospheric Observatory. $NO_2$ was quantified in a second channel by photolytic conversion to NO using blue light LED diodes centred at 395nm. The 395nm wavelength has a specific affinity for $NO_2$ photolytic conversion to NO, giving high analyte selectivity within the channel. Recent work (Pollack et al., 2010) evaluated the relative high $NO_2$ affinity for conversion of $NO_2$ to NO using 395nm blue light LED's. They highlighted the low probability of other species

within the gaseous chemical matrices such as nitrous acid (HONO), being affected by the 395nm light, so in turn reducing possible non $NO_2$ species interfering with the measurement. $NO_x$ was then quantified by ozonation of the subsequent total NO present in the reaction vessel after conversion with $NO_2$ derived from the difference between $NO_x$ and NO mixing ratios.

The instrument was calibrated by adding a small flow (5 sccm) of a known NO concentration (5 ppmv – Air Liquide) in the ambient sample flow, resulting in around 10ppbv of NO. The conversion efficiency of the $NO_2$ converter was measured during each calibration by gas phase titration of the NO to $NO_2$ by addition of $O_3$. $NO_2$ mixing ratio data is corrected for using the measured 90% photolytic conversion efficiency. In flight calibrations were always carried out above the boundary layer, thus ensuring low and stable background levels of $NO_x$. Typically calibrations are carried out at the beginning and end of a flight, with sensitivities and conversion efficiency interpolated between the two and applied to all data. In this work, the 10Hz data has been averaged to 1Hz, with detection limits for the 1Hz data being ~75pptv for NO and 100pptv for $NO_2$ with approximate total errors at 1ppbv being 10 and 15% for NO and $NO_2$ respectively.

## 2.5 Ozone sampling

Ozone was quantified in-situ, using a Thermo Scientific 49i UV absorption instrument generating data every 4 seconds. A mercury lamp emitting UV light was used, with absorption at 254 nm being proportional to $O_3$ concentration. The measurement uncertainty was estimated to be ±0.8 ppbv.

## 2.6 VOC sampling

Benzene and toluene mixing ratios were determined simultaneously using an Ionicon (Innsbruck, Austria) high sensitivity proton transfer reaction mass spectrometer (PTR-MS) fitted with a stainless steel ringed drift tube (9.6 cm) and three Pfieffer turbo-molecular pumps. This instrument has been described in detail elsewhere (Karl et al., 2009;de Gouw and Warneke, 2007;Hewitt et al., 2003;Hayward et al., 2002). Therefore only instrument setup, operation and flight modifications are outlined here. The instrument, normally housed in one cabinet, had been re-engineered by the manufacturers into two racks suitable for mounting into the aircraft. To mitigate shock and vibration to the PTR-MS during flight, the instrument racks, mass spectrometer and MD4 diaphragm pump were individually shock

mounted using stainless steel spring mountings (vibrachoc). A pressure controller was added (Bronkhorst) which regulates the inlet flow (50-500 sccm), such that pressure upstream of the controller is maintained at a constant value. As a result the PTR-MS drift tube pressure is independent of fluctuations in ambient pressure caused by varying flight altitude. Ambient sample air was only exposed to heated (70°C) Teflon and stainless steel tubing, minimizing memory effects, inlet losses and the build-up of impurities in the inlet system. Considerable efforts were made to prevent VOC contamination of the PTR-MS inlet during operation on the ground and during take-off. On the ground the PTR-MS inlet remained closed (and all sample tubing capped). Approximately 3 hours before each flight the instrument voltages were switched on to allow for primary ion count stabilisation and instrument calibration. During this time dry zero grade air (BOC) was purged through the zero air generator and PTR-MS inlet in series to minimise instrument background and to prevent the build-up of contaminants. Immediately prior to take off, the sample flow was instantaneously switched to dry zero grade air contained in a 1L silica coated stainless-steel can (Thames Restek, UK) within the aircraft, which was then continuously sampled until the aircraft had reached an altitude of 2500m, allowing the PTR-MS to be fully operational during take-off.

VOC measurements were obtained at a sampling rate of 5 Hz and a repetition rate of ~2 Hz. In this work, the 2Hz mixing ratios data has been averaged to 1Hz for analysis. The target protonated masses and likely contributing compounds were *m/z* 79 (benzene) and *m/z* 93 (toluene). Additionally, both the primary ion count *m/z* 21 ($H_3{}^{18}O^+$), its first water cluster ($H_3{}^{18}O\ H_2{}^{18}O^+$) at *m/z* 39 and $O_2{}^+$ at *m/z* 32 were determined. PTR-MS drift tube pressure, temperature and voltage were held constant at 2.0 mbar, 40°C and 480 V respectively, maintaining an E/N ratio of approximately 110 Td. For flights at ~360 m a.g.l, the *m/z* 21 primary ion count ranged between (4 – 7) x $10^7$ ion counts per second (cps) with an average of 6 x $10^7$. Ion counts of *m/z* 32 ranged between (0.8 – 3) x $10^6$ cps, with an average of 2 x $10^6$ cps, which represented 3% of the primary ion signal. Ion counts of *m/z* 39 ranged between (1 – 5) x $10^6$ cps with an average of 3 x $10^6$ cps, which represented 6% of the primary ion signal.

Toluene and benzene calibrations were carried out approximately 2 hours prior to each flight using an in-house built dynamic dilution calibration system. This involved the dynamic dilution of a 500 ppbv certified gas standard (Apel, Riemer) with humidity controlled zero grade air (BOC gases) to mixing ratios near typically observed levels. Zero air humidity was

calibrated over 20 -80% RH in triplicate to assess humidity effects on sensitivity during the campaign. Benzene and toluene do not react with the hydrated hydronium ions generated at higher ambient air humidity within the PTRMS drift tube (Warneke et al., 2001). To account for this humidity dependent PTRMS sensitivity toward benzene and toluene, these compounds were normalised against the hydronium ion counts only. Typical instrument sensitivities observed during the campaign ranged between 380 – 480 icps $ppbv^{-1}$, 6 – 8 normalised ion counts per second (ncps), and 400 – 600 icps $ppbv^{-1}$, 6 – 9 ncps, for benzene and toluene respectively. Instrument uncertainties were 16±5 and 21±9 % for benzene and toluene respectively, calculated using the standard deviation of linear regression (Sm) of pre-flight calibrations. Instrument limits of detection (LoDs) for 1Hz averaged data were determined by the method outlined by Taipale and colleagues (Taipale et al., 2008) and were 13±8 and 18±11pptv for benzene and toluene respectively.

During flights, ambient air was sampled from the forward facing stainless steel isokinetic inlet along a heated (70°C) 5 m ¼" Teflon tube (0.21" ID) pumped by a stainless steel diaphragm pump (Millipore) at a flow-rate of 22L $min^{-1}$. A portion of this ambient air (~300 sccm) was diverted into the pressure controlled inlet of the PTR-MS instrument such that the overall delay time was < 3 s. To determine blank VOC mixing ratios, the remaining ambient air was purged into a custom built zero air generator which consisted of a 3/8" stainless steel tube packed with 1g of platinum coated quartz wool (Elemental Microanalysis) which efficiently removes VOCs (de Gouw et al., 2004). The zero air generator was operated at 350°C and 30 psi for the duration of the flights to maintain optimal operating conditions. The catalytic converter does not remove water vapour from the sample stream, which is of particular importance as the instrument response from background impurities may depend upon sample air humidity. During flights, zero air was periodically back-flushed through the inlet system to determine instrument background.

## 2.7 LAQN ground monitoring sites

Data were obtained from three LAQN ground level monitoring sites for comparative purposes. These were:

(i) Marylebone Road (Westminster), an urban kerbside site in a street canyon, situated 1.5 m from the kerb of a frequently congested 6 lane road, the A501 (51.5225°N, 0.1546°W).

(ii) Horseferry Road (Westminster), an urban background monitoring station located within an area of mixed commercial and residential buildings (51.4947°N, 0.1319°W). The nearest road is the B323 Horseferry Road approximately 17 m north of the station.
(iii) Greenwich-Eltham (Eltham), a suburban background site situated in Greenwich within an education centre (51.4526°N, 0.0708°E). The site is approximately 25 m from the nearest road, the A210 Bexley Road. The surrounding area consists of trees, grassland, recreational areas and suburban housing.

These sites all monitor NO, $NO_2$ and $NO_x$ at hourly resolution and $O_3$ at 15 minute resolution. However, only the Westminster-Marylebone Road and Greenwich-Eltham monitoring sites monitor benzene and toluene at hourly resolution. The locations are shown in figure S-1.

## 3 Results

### 3.1 Intercomparison of WAS TD-GCFID and PTR-MS

To compare the volume mixing ratios obtained with the on-board PTR-MS with those measured by gas chromatography with flame ionisation detection (GC-FID), whole air canister sampling (WAS) was conducted twice per flight using silica coated stainless steel cans (Thames Restek, UK) with subsequent GC-FID analysis for benzene and toluene (Hopkins et al., 2009;Hopkins et al., 2003). The WAS system avoids possible artefact formation or analyte loss that may occur on adsorbents if a pre-concentration sampling system is used (Cao and Hewitt, 1993, 1994a, b). Previous ground observations in several urban environments have shown generally good agreement between benzene and toluene mixing ratios obtained during PTR-MS and GC-FID intercomparisons (Rogers et al., 2006;Warneke et al., 2001). However (Jobson et al., 2010) suggest a 16% overestimation of benzene mixing ratios determined by PTR-MS compared to a GC method, attributed to the fragmentation of higher alkyl-benzenes (eg ethyl-benzene). Inter-comparison of the two sampling methods showed excellent agreement within uncertainty and in particular suggest that the PTR-MS demonstrated minimal bias due to the fragmentation of higher alkyl benzenes during this study, as shown figure S-2. Hence the PTR-MS signal obtained at m/z 79 is assumed to be due to benzene alone.

### 3.2 Interpretation of temporal trace gas profiles

Mixing ratios of VOCs, $NO_x$, $O_3$ and $NO/NO_2$ ratios from 27 individual flight-transects of Greater London during RF 2 – 6 were averaged to assess how they changed with respect to

time over the 7 days of flights, table 2. As shown in figure 2, $NO_x$, benzene and toluene mixing ratios followed the typical diurnal pattern previously observed in urban areas with measured maxima during morning rush hours and a measured minimum at approximately 16:00 – 18:00 when $O_3$ reaches its maximum (Langford et al., 2010;Marr et al., 2013). The highest $NO_x$ and VOC mixing ratios were observed in the morning at 10:30 local time, ~ 40 ppbv $NO_x$, ~350 pptv toluene and ~200 pptv benzene at 360±10 m a.g.l., when emissions from traffic related sources are highest and the mixing height relatively low. Mixing ratios decreased throughout the morning, probably due to a combination of boundary layer development leading to dilution and increasing OH oxidation leading to enhanced chemical removal, with mixing ratios stabilising later in the day at 10 – 20 ppbv $NO_x$ and between 90 – 150 pptv benzene and toluene. Variations in $O_3$ mixing ratio are generally attributed to photochemical production in the mixing layer with some contribution from entrainment from the free troposphere (Dueñas et al., 2002). In London, the low $O_3$ morning mixing ratios were attributed to the destruction of $O_3$ by rapid titration with NO, which is emitted during the morning rush hour and highest during the morning. As the day progresses, sunlight intensity becomes higher increasing the radical concentration and hence NO to $NO_2$ oxidation rate from the reaction of NO with peroxy radicals. Subsequent photolysis of $NO_2$ leading to increased $O_3$ throughout the day (Pudasainee et al., 2010), with this rate of $O_3$ production being a function of $NO_x$ and VOC levels as well as sunlight intensity.

Recent studies of annually averaged daily VOC mixing ratios in London from the 191 m high BT Tower have shown that benzene and toluene mixing ratios typically display two day-time maxima, one occurring around 9:00 and a second larger peak occurring between 18:00 and 21:00 coinciding with morning and evening peak traffic periods (Langford et al., 2010;Lee et al., 2015). $NO_x$ mixing ratios are highest when traffic flow peaks, with higher $O_3$ mixing ratios corresponding to lower $NO_x$ mixing ratios and vice versa during a 24 hour period (Im et al., 2013;Lu and Wang, 2004;Mazzeo et al., 2005). This indicates that patterns in VOC and $NO_x$ emission have a larger effect on observed mixing ratios in the boundary layer than does boundary layer dynamics.

### 3.3 Horizontal spatial distribution of VOCs and $NO_x$ mixing ratios

The predominant wind directions observed during the flights were north-westerly (RF 2-6), perpendicular to the flight transects, (table 1). Research flights 2-6 were used to provide a

cross section of pollutant mixing ratios across London. The relative spatial distribution of VOC and $NO_x$ mixing ratios across greater London during these flights were superficially consistent, with average mixing ratios for each flight leg only changing temporally (figure 2), hence only RF 5 is shown here.

Figures 3 and 4 show 1 km averaged mixing ratios of VOCs and $NO_x$ respectively during RF 5 against latitude across Greater London. Both VOCs and $NO_x$ mixing ratios show significantly higher mixing ratios in inner London. For all compounds the highest mixing ratios were observed within inner London at 360±10 m a.g.l. particularly directly downwind of the London CCZ. Average mixing ratios observed within inner London were 0.20±0.05, 0.28±0.07, 13.2±8.6, 21.0±7.3 and 34.3±15.2 ppbv for benzene, toluene, NO, $NO_2$ and $NO_x$ respectively. Mixing ratios for benzene, toluene, NO, $NO_2$ and $NO_x$ for all flights are shown in table 2.

Vehicular emissions are considered to be an important source for VOCs and $NO_x$ in Greater London (Langford et al., 2010;Lee et al., 2015). Toluene has a shorter atmospheric lifetime than benzene due to faster photochemical removal by OH (rate constants of $1.45\pm0.06 \times 10^{12}$ *k*, $cm^3$ $molecule^{-1}$ $s^{-1}$; $6.03\pm0.17 \times 10^{12}$ *k*, $cm^3$ $molecule^{-1}$ $s^{-1}$ for benzene and toluene respectively at 298 K; (Ohta and Ohyama, 1985)), thus the T/B ratio can indicate the photochemical age of the pollution carried by air masses (Warneke et al., 2001;Atkinson, 2000). Very close to the source of emissions (e.g. at the kerbside), the ratio of VOC mixing ratios should be similar to those in the emissions themselves. As toluene is more rapidly removed by oxidation, the T/B ratio progressively decreases as air is transported over longer distances away from the source. Vehicular exhaust emission ratios from combustion during transient engine operation is dependent on gasoline composition but within Europe typically yield T/B ratios between 1.25 – 2.5 ppbv $ppbv^{-1}$ (Heeb et al., 2000). The introduction of catalytic converters to vehicular exhausts significantly has been shown to decrease this T/B ratio, attributed to the reduced catalytic conversion efficiency for benzene with respect to alkylated benzenes (Heeb et al., 2000). Hence observed ambient T/B mixing ratios will be a product of the photo-chemical age of the air mass since emission, vehicular fleet composition, gasoline composition and the ratio of vehicles using catalytic converters.

Recent long-term VOC measurements made at two ground level sites in central London dominated by traffic sources, Marylebone Road and North Kensington (Valach et al., 2014), showed average T/B ratios of 1.6±0.3 ppbv $ppbv^{-1}$ and 1.8±0.3 ppbv $ppbv^{-1}$ respectively.

These T/B ratios are similar to the average T/B concentration ratio of 1.8 ± 0.5 ppbv $ppbv^{-1}$ observed within inner London in this study, where traffic sources are likely to be the highest (figure 3). Average T/B concentration ratios in suburban (latitude 51.30 – 51.35°) and south-western Greater London (latitude 51.35 – 51.42°) were 1.1 ± 0.3 ppbv $ppbv^{-1}$ and 1.3 ± 0.4 ppbv $ppbv^{-1}$ respectively. This could be interpreted as increasing air mass age from emission and suggests that the sources of benzene and toluene in these regions are likely the product of local emission and horizontal advection from inner London.

Linear regression analysis between NO, $NO_2$ $NO_x$, benzene and toluene mixing ratios yielded correlation coefficients ($R^2$) ranging between 0.12 and 0.64. The weakest linear regressions were observed between toluene and NO ($R^2$ = 0.12, n = 7500) and benzene and NO ($R^2$ = 0.14, n = 6500), not shown. The strongest linear regressions were observed between toluene and benzene ($R^2$ = 0.51, n = 6500) and toluene and $NO_2$ ($R^2$ = 0.64, n = 7500) (figure 5). A strong covariance exists between benzene, toluene and $NO_2$ mixing ratios indicating that these compounds potentially share the same or co-located sources within the Greater London area, most likely vehicular emission. However the measured $NO_2$/NO concentration ratio at 360m a.g.l is likely to be dominated by photochemistry rather than emission sources (Atkinson et al.2000).

Figure 5 also suggests a secondary source contribution to toluene that is not shared with $NO_2$ or benzene and hence is not related to traffic emissions. This secondary source is localised to a discrete peak in observed toluene in SE London within the borough of Lambeth (latitude 51.455°, longitude -0.141°). This was observed during three of the seven flight transects in which toluene mixing ratios at 360±10 m a.g.l. increased from 0.25 ppbv to 0.6 ppbv with a T/B ratio of up to 3 ppbv $ppbv^{-1}$, as seen in figure 3. Toluene has numerous anthropogenic sources including evaporative fuel losses, industrial solvents, paint thinners and the manufacturing of ink and paints. Direct toluene emissions from industrialised areas in Mexico city with T/B ratios of up to 8.5 - 12.5 ppbv $ppbv^{-1}$ have previously been reported (Karl et al., 2009). In the absence of any identifiable industrialised areas upwind of the region of high T/B ratios in Lambeth, this peak is possibly due to the horizontal advection of industrial emissions from outside of London, or some unidentified localised source of toluene.

The influence of $NO_x$ and VOC emission from London Heathrow Airport (LHA) during this study was investigated with plume dispersion modelling using the NOAA Hybrid Single-Particle Lagrangian Integrated Trajectory (HYSPLIT) model. The model isolates the region of the flight track influenced by potential pollutant outflow from LHA during the flight. Four hour averaged forward dispersion forecasting from LHA was modelled for RF1 and RF5 between 14:00 – 16:00 and 9:00 – 12:00 local time respectively. The lower and upper limits of the averaged dispersion layer were 300 – 400m agl, similar to the measured average flight altitudes during these flights. During RF1 and RF 5 the transport time from LHA to the flight transect was approximately 25-50 minutes, calculated from the average observed horizontal wind speed and the ~20 km downwind distance (figure 6).

Figure 6 shows the region of flight transects which were influenced by LHA outflow (51.39 – 51.45° latitude). On entering the LHA outflow plume, $NO_x$ mixing ratios at 360±10 m a.g.l. during both RF1 and RF5 were observed to double increasing from ~15 to 30 ppbv, suggesting a strong $NO_x$ source. As shown in figure 4 for RF5, the $NO/NO_2$ ratio also gradually increased across the plume from 0.5 up to 0.8 ppbv $ppbv^{-1}$, which is consistent with previous studies that have found higher NO mixing ratios in aircraft exhaust (Spicer et al., 1994;Schäfer et al., 2000). Toluene and benzene mixing ratios showed a negligible increase from ~0.20 – 0.26 and ~0.15 – 0.18 ppbv at 360±10 m a.g.l. across the plume respectively, with T/B ratios of 1.5 - 1.7 ppbv $ppbv^{-1}$ indicative of vehicular exhaust emission as the dominant VOC source. Previous ground observations (Carslaw et al., 2006) at LHA suggested that approximately 27% of the annual mean $NO_x$ and $NO_2$ were due to airport operations at the airport boundary. At background locations 2–3 km downwind of the airport they estimated that the upper limit of the airport contribution to be less than 15%. Our measurements are in qualitative agreement with this study, suggesting that even though Heathrow is an important emission source of $NO_x$, observed mixing ratios of $NO_x$ close to the airport are dominated by road traffic sources. As LHA was ~ 20 km upwind of the flight transects, our observed mixing ratios are likely to be heavily influenced by emissions during advection from LHA to the measurement locations and as such conclusions drawn from this data is tentative.

### 3.4 Interpretation of vertical trace gas profiles

To date the influence of vertical transport on the distribution of trace gases in the urban boundary layer has primarily been studied with respect to vertical profiles of ozone, which are typically with in-situ instruments mounted on tethered balloons (Beyrich et al., 1996;Güsten et al., 1998;Newchurch et al., 2003). Vertical profiling of VOCs, NO, $NO_2$ and $NO_x$ have also been studied using a combination of in-situ measurements from tethered balloons and ground based differential optical absorption spectroscopy (DOAS) over several American (Wang et al., 2003;Stutz et al., 2004;Velasco et al., 2008;Hu et al., 2012) and European cities (Glaser et al., 2003). To the author's knowledge, the work herein represents the first vertical boundary layer profiling of both VOCs and $NO_x$ species using research aircraft over a European city.

Vertical profiling of VOCs, $NO_x$ and $O_3$ above Greater London in this study was conducted during RF 1 on 24/6/13 between the hours of 17:00 -18:00 local time. Vertical profiling consisted of three sequentially stacked flights conducted at 350 m agl (17:00 – 17:20), 510 m agl (17:20 – 17:40) and 650 m agl (17:40 – 18:00). The trace gas mixing ratios observed at each altitude were then averaged along the ~35 km flight path over Greater London. These concentration profiles were then compared with hourly averaged upwind LAQN kerbside measurements made at 17:00 from the Marylebone Road air quality monitoring station to interpret how trace gas mixing ratios change vertically from the street canyon to above the urban canopy. At its closest point, flight legs were ~ 6 km downwind of the Marylebone Road measurement site. During RF 1, a predominantly north westerly wind direction was observed with a mean wind direction and wind speed of 285.9±17.1° and 13.6 m/s respectively. Hence, the vertical concentration profiles observed represents a composite of local emission and horizontal advection of the Greater London region.

Figure 7 shows the comparison between the measured trace gas concentration profiles over Greater London and the Marylebone Road kerbside measurements. The measured concentration distributions of both benzene (0.15 ± 0.01 ppbv) and toluene (0.16 ± 0.01 ppbv) and their corresponding T/B ratio (1.1 ± 0.3 ppbv $ppbv^{-1}$) were vertically uniform with increasing altitude, suggesting rapid mixing between 350 – 650 metres. In this case VOC losses due to reaction with the OH radical are evidently too slow to produce observable concentration gradients in the vertical distribution. This suggests that turbulence mixes the species up to 650 m agl much faster than the OH radical depletes them. Over urban areas

turbulence is promoted throughout the day due to thermal forcing produced by the urban energy balance (Velasco et al., 2008).

Both NO and $NO_2$ show a large decrease in mixing ratios between measurements at the kerbside and at 360±10 m a.g.l. (43 and 4.4 ppbv for NO respectively and 28 and 17ppbv for $NO_2$). In contrast to NO and $NO_2$, $O_3$ measurements were lowest at the kerbside site, 17 ppb, increasing to 32 ppbv at 360±10 m a.g.l. The daytime vertical profiles of NO, $NO_2$ and $O_3$ are caused due to a combination of turbulent mixing and three main simultaneous competing effects. The chemical production of $NO_2$ by NO titration with $O_3$ and $RO_2$, causing higher $NO_2$ and lower $O_3$ mixing ratios closer to the surface due to higher surface NO mixing ratios. Photochemical production of NO and $O_3$ from $NO_2$ and subsequent $O_3$ destruction. $NO_2$ and ozone dry deposition processes which dominate closer to the surface (Wesely and Hicks, 2000).

The vertical profiles of $NO_x$ and $O_3$ are superficially anti-correlated with altitude. The observed $O_3$ profiles, with lower values close to the ground and higher values aloft, agree in their general behaviour with other observations (Beyrich et al., 1996;Glaser et al., 2003;Güsten et al., 1998) The vertical profiles of $O_3$ and $O_x$ (the sum of $O_3$ and $NO_2$) show the importance of NO emission for $O_3$ depletion, with reduced surface $O_3$ mixing ratios closer to the ground largely compensated by a corresponding increase in $NO_2$. As a result, $O_x$ exhibits a very uniform vertical concentration between 350 – 650 m agl. However, $O_x$ mixing ratios are reduced at ground level possibly due to enhanced deposition in proximity to the surface.

### 3.5 Comparison of airborne measurements with LAQN ground sites

Data obtained from three LAQN air quality ground monitoring stations located in three typical urban environments (urban kerbside: Marylebone Road; urban background: Westminster-Horseferry Road; and suburban background: Greenwich-Eltham) were compared against airborne mixing ratios at 360±10 m a.g.l. to assess how $O_3$ and its precursors are distributed across the city. Dispersion modelling using the NOAA HYSPLIT model was used to highlight regions of the flight track most influenced by pollutant outflow from each of the ground monitoring stations. Briefly, four hour averaged forward and reverse dispersion forecasting was modelled for Marylebone Road, Westminster and Eltham respectively during flights with a prevailing north westerly wind direction (RF 1, RF4 - 6,

table 1). RF 2 and 3 were not used in the comparison due to low observed wind speeds, < 5 m $s^{-1}$. The lower and upper limits of the averaged dispersion layer were 300 – 400 m agl, similar to the measured average flight altitude of 360±10 m a.g.l during RF 1, RF4 - 6. Airborne mixing ratios for comparison were given as the arithmetic average and 1 standard deviation of the hourly measurements within the dispersion plume. The approximate transport times from Marylebone Road, Westminster and Eltham to the flight transect ranged between 3 – 7, 7 – 15 and 14 – 28 minutes respectively, calculated from the observed horizontal wind speed and the downwind/upwind distance for each ground station during each flight (figure S-1).

Figure 8 shows a linear regression analysis between airborne and ground mixing ratios of benzene, toluene, NO, $NO_2$, $NO_x$ and $O_3$. Strong positive correlations are observed for all species at all three ground sites with $R^2$ values ranging from 0.54 – 0.97 (n = 7). Ground mixing ratios of both VOCs and $NO_x$ species were significantly higher at the Marylebone Road kerbside site relative to the urban background (Westminster) and suburban background (Eltham) sites. Average mixing ratios observed at ground level for benzene and toluene respectively were 0.12±0.05; 0.21±0.08 ppbv at Marylebone Road and 0.07±0.01; 0.13±0.03 ppbv at Eltham, with T/B ratios of 1.7-1.8 ppbv $ppbv^{-1}$ indicative of vehicular emissions as the dominant source at both sites. $NO_x$ mixing ratios were also significantly higher at Marylebone Road (121.96±45.28 ppbv) than Westminster (40±4.45 ppbv) and Eltham (10.02±4.28). For $O_3$, the mean mixing ratios observed at Westminster (13.56±4.9 ppbv) were lower than at Eltham (19.14 ± 3.2 ppbv) whilst the lowest mixing ratios were at the Marylebone Road site (9.23±8.42 ppbv). The $O_3$ mixing ratios at these sites are anti-correlated to that of NO (figure 8), through enhanced NO emission and subsequent titration of $O_3$ in proximity to busy road networks.

Also of interest, $NO/NO_2$ ratios were higher at the Marylebone Road site (0.62±0.25) than at Westminster (0.50±0.15) and Eltham (0.25±0.09). Historically, vehicular diesel and petrol emissions of NOx were dominated by emissions of NO ($NO/NO_2$ ratios of 0.9 ≤). However, recent developments in diesel emission technology, specifically diesel oxidation catalysts and particulate filters, have caused significant increases in direct vehicular $NO_2$ emissions in the UK and Europe. Current diesel emission control technology deliberately produces enhanced $NO_2$ mixing ratios to oxidise and reduce black carbon particulates in the vehicular exhaust gas (Carslaw and Rhys-Tyler, 2013). Increasing numbers of diesel vehicles in Central London with this emission reduction technology could have contributed to the low $NO/NO_2$

ratios observed from all three ground air monitoring stations observed during this study. This is in good agreement with the observed covariance of benzene, toluene and $NO_2$ mixing ratios shown in figure 5, potentially indicating these species have common sources, most likely from vehicular emission. However the measured $NO/NO_2$ concentration ratio at 360m a.g.l is likely to be dominated by photochemistry rather than emission sources (Atkinson et al.2000).

Airborne mixing ratios of $O_3$ were consistently higher than those at ground level, consistent with the ground surface in London acting as a chemical sink for $O_3$, which is in good agreement with the measured vertical profile of $O_3$ shown in figure 7. Mixing ratios of the selective VOC and $NO_x$ species observed at the roadside site at Marylebone Road were significantly higher than those of the airborne measurements. Assuming this difference is due entirely to mixing, this reduction in mixing ratio crudely indicates a dilution factor of 2 - 6 between the roadside site in the Marylebone Road and the 355 m sampling point. This agrees well with comparisons made during REPARTEE I which concluded a dilution factor of ~5 for $NO_x$ mixing ratios between Marylebone Road and the 190 m sampling point on the BT tower (Harrison et al., 2012), well above the surrounding building height. Dilution factors for VOC and NOx species at Westminster and Eltham ranged between 0.46 – 2.34 which are significantly lower than those observed at Marylebone Road. This difference in dilution factors is largely due to firstly the Marylebone Road measurement site being in central London, a very large source of VOCs and $NO_x$ and being closest in proximity to the 6 lane frequently congested road. Secondly Marylebone Road is within an urban street canyon whose orientation serves to maximise mixing ratios of emissions therein. Street canyons are not as well ventilated as with more open locations such as urban and suburban sites which tends to result in increased surface mixing ratios (Pugh et al., 2012;Carslaw and Rhys-Tyler, 2013) .

## 4 Conclusions

Measurements of VOCs, $NO_x$ and $O_3$ in the boundary layer were made in transects across Greater London at 360±10 m a.g.l. during the summer of 2013, with a view to identifying the dominant $O_3$ precursor sources within the region, and to better understanding the effects of chemical interactions between these pollutants and meteorological variables on urban air quality. Observed benzene, toluene and $NO_x$ mixing ratios across Greater London were mostly due to traffic emissions, with the highest mixing ratios observed over inner London,

where the density of traffic and other pollutant sources is higher than over outer London. The highest T/B ratios (1.8 ± 0.5 ppbv ppbv$^{-1}$) observed within inner London is indicative of local vehicular sources. Linear regression analysis of VOC and $NO_x$ species which showed a covariance between benzene, toluene and $NO_2$ mixing ratios, potentially indicating that their dominant sources are the same or are co-located throughout London. Modern diesel vehicles use emission control technology to reduce black carbon emissions but which also enhance the $NO_2$/NO ratio in the vehicle exhaust (Carslaw and Rhys-Tyler, 2013). As the measured NO/$NO_2$ concentration ratio at 360m .a.g.l. is likely to be dominated by photochemistry rather than emission sources, VOCs correlate well with $NO_2$ but not NO due to its longer atmospheric lifetime (Atkinson et al.2000).

Airborne mixing ratios were compared to kerbside data from three LAQN air quality ground monitoring stations within Greater London. Strong positive correlations were observed for $O_3$, NO, $NO_2$, $NO_x$, benzene and toluene species at all three ground sites with $R^2$ values ranging from 0.54 – 0.97 (n = 7) suggesting that airborne mixing ratios were characteristic of surface mixing ratios during the analysis period. $NO_x$ and VOC mixing ratios observed at the Marylebone Road air quality monitoring site were 2 – 6 times higher than those observed at 360±10 m a.g.l due to a combination of its proximity to the emission sources, photochemical aging and dilution of the air mass during vertical mixing.

An increase in $NO_x$ mixing ratios from ~15 to 30 ppbv at 360±10 m a.g.l. during RF1 and RF5 was observed ~20 km downwind of LHA. Our measurements tentatively support previous studies that suggest that even though Heathrow is an important emission source of $NO_x$, observed mixing ratios of $NO_x$ even quite close to the airport are dominated by road traffic sources. Since LHA was ~ 20 km upwind of the flight transects, these observed mixing ratios are likely to be heavily influenced by vehicular emissions during advection from LHA to the measurement location.

## Author contribution

MD Shaw and JD Lee redesigned the PTR-MS and NOx chemiluminescence instruments for the aircraft. MD Shaw, JD Lee, A Harvey and B Davison designed the field experiment and carried it out. MD Shaw, JD Lee, A Vaughan, RM Purvis, AC Lewis and CN Hewitt were responsible for analysis/interpretation of the data.

## Acknowledgements

We thank the UK Natural Environment Research Council (grant NE/J00779X/1) and the Department of Environment, Food and Rural Affairs for funding We thank Captain Carl Joseph, co-pilot James Johnson and instrumental engineer Thomas Millard (ARSF) for their expert support during the flights and James Hopkins and Shallini Punjabi (National Centre for Atmospheric Science, University of York, UK) for the WAS TD-GC-FID benzene and toluene concentration data.

## References

Atkinson, R.: Atmospheric chemistry of VOCs and NOx, Atmospheric Environment, 34, 2063-2101, 2000.

Beswick, K., Gallagher, M., Webb, A., Norton, E., and Perry, F.: Application of the Aventech AIMMS20AQ airborne probe for turbulence measurements during the Convective Storm Initiation Project, Atmos. Chem. Phys, 8, 5449-5463, 2008.

Beyrich, F., Weisensee, U., Sprung, D., and Güsten, H.: Comparative analysis of sodar and ozone profile measurements in a complex structured boundary layer and implications for mixing height estimation, Boundary-Layer Meteorology, 81, 1-9, 1996.

Cao, X.-L., and Hewitt, C. N.: Thermal desorption efficiencies for different adsorbate/adsorbent systems typically used in air monitoring programmes, Chemosphere, 27, 695-705, 1993.

Cao, X.-L., and Hewitt, C. N.: Study of the degradation by ozone of adsorbents and of hydrocarbons adsorbed during the passive sampling of air, Environmental Science & Technology, 28, 757-762, 1994a.

Cao, X.-L., and Hewitt, C. N.: Build-up of artifacts on adsorbents during storage and its effect on passive sampling and gas chromatography-flame ionization detection of low concentrations of volatile organic compounds in air, Journal of Chromatography A, 688, 368-374, 1994b.

Carslaw, D. C., Beevers, S. D., Ropkins, K., and Bell, M. C.: Detecting and quantifying aircraft and other on-airport contributions to ambient nitrogen oxides in the vicinity of a large international airport, Atmospheric Environment, 40, 5424-5434, 2006.

Carslaw, D. C., and Rhys-Tyler, G.: New insights from comprehensive on-road measurements of $NO_x$, $NO_2$ and $NH_3$ from vehicle emission remote sensing in London, UK, Atmospheric Environment, 81, 339-347, 2013.

de Gouw, J., Warneke, C., Holzinger, R., Klüpfel, T., and Williams, J.: Inter-comparison between airborne measurements of methanol, acetonitrile and acetone using two differently configured PTR-MS instruments, International Journal of Mass Spectrometry, 239, 129-137, 2004.

de Gouw, J., and Warneke, C.: Measurements of volatile organic compounds in the earth's atmosphere using proton-transfer-reaction mass spectrometry, Mass Spectrometry Reviews, 26, 223-257, 2007.

Dueñas, C., Fernández, M., Cañete, S., Carretero, J., and Liger, E.: Assessment of ozone variations and meteorological effects in an urban area in the Mediterranean Coast, Science of the Total Environment, 299, 97-113, 2002.

Glaser, K., Vogt, U., Baumbach, G., Volz-Thomas, A., and Geiss, H.: Vertical profiles of $O_3$, $NO_2$, $NO_x$, VOC, and meteorological parameters during the Berlin Ozone Experiment (BERLIOZ) campaign, Journal of Geophysical Research: Atmospheres (1984–2012), 108, 2003.

Güsten, H., Heinrich, G., and Sprung, D.: Nocturnal depletion of ozone in the Upper Rhine Valley, Atmospheric Environment, 32, 1195-1202, 1998.

Harrison, R., Dall'Osto, M., Beddows, D., Thorpe, A., Bloss, W., Allan, J., Coe, H., Dorsey, J., Gallagher, M., and Martin, C.: Atmospheric chemistry and physics in the atmosphere of a developed megacity (London): an overview of the REPARTEE experiment and its conclusions, Atmospheric Chemistry and Physics, 12, 3065-3114, 2012.
Hayward, S., Hewitt, C., Sartin, J., and Owen, S.: Performance characteristics and applications of a proton transfer reaction-mass spectrometer for measuring volatile organic compounds in ambient air, Environmental Science & Technology, 36, 1554-1560, 2002.
Heeb, N. V., Forss, A.-M., Bach, C., Reimann, S., Herzog, A., and Jäckle, H. W.: A comparison of benzene, toluene and $C_2$-benzenes mixing ratios in automotive exhaust and in the suburban atmosphere during the introduction of catalytic converter technology to the Swiss Car Fleet, Atmospheric Environment, 34, 3103-3116, 2000.
Hewitt, C., Hayward, S., and Tani, A.: The application of proton transfer reaction-mass spectrometry (PTR-MS) to the monitoring and analysis of volatile organic compounds in the atmosphere, Journal of Environmental Monitoring, 5, 1-7, 2003.
Hopkins, J. R., Lewis, A. C., and Read, K. A.: A two-column method for long-term monitoring of non-methane hydrocarbons (NMHCs) and oxygenated volatile organic compounds (o-VOCs), Journal of Environmental Monitoring, 5, 8-13, 2003.
Hopkins, J. R., Evans, M. J., Lee, J. D., Lewis, A. C., Marsham, J., McQuaid, J., Parker, D. J., Stewart, D. J., Reeves, C. E., and Purvis, R. M.: Direct estimates of emissions from the megacity of Lagos, Atmospheric Chemistry and Physics, 9, 8471-8477, 2009.
Hu, S., Paulson, S. E., Fruin, S., Kozawa, K., Mara, S., and Winer, A. M.: Observation of elevated air pollutant concentrations in a residential neighborhood of Los Angeles California using a mobile platform, Atmospheric Environment, 51, 311-319, 2012.
Im, U., Incecik, S., Guler, M., Tek, A., Topcu, S., Unal, Y. S., Yenigun, O., Kindap, T., Odman, M. T., and Tayanc, M.: Analysis of surface ozone and nitrogen oxides at urban, semi-rural and rural sites in Istanbul, Turkey, Science of the Total Environment, 443, 920-931, 2013.
Jobson, B. T., Volkamer, R., Velasco, E., Allwine, G., Westberg, H., Lamb, B. K., Alexander, M., Berkowitz, C. M., and Molina, L. T.: Comparison of aromatic hydrocarbon measurements made by PTR-MS, DOAS and GC-FID during the MCMA 2003 Field Experiment, Atmospheric Chemistry and Physics, 10, 1989-2005, 2010.
Kansal, A.: Sources and reactivity of NMHCs and VOCs in the atmosphere: A review, Journal of hazardous materials, 166, 17-26, 2009.
Karl, T., Apel, E., Hodzic, A., Riemer, D., Blake, D., and Wiedinmyer, C.: Emissions of volatile organic compounds inferred from airborne flux measurements over a megacity, Atmos. Chem. Phys, 9, 271-285, 2009.
Langford, B., Nemitz, E., House, E., and Phillips, G.: Fluxes and concentrations of volatile organic compounds above central London, UK, Atmospheric Chemistry and Physics, 2010.
Lee, J., Moller, S., Read, K., Lewis, A., Mendes, L., and Carpenter, L.: Year-round measurements of nitrogen oxides and ozone in the tropical North Atlantic marine boundary layer, Journal of Geophysical Research, 114, D21302, 2009.
Lee, J., Helfter, C., Purvis, R., Beavers, S., Carslaw, D., Lewis, A., Moller, S., Nemitz, E., and Tremper, A.: Measurement NOx fluxes from a tall tower above central London, UK and comparison with emissions inventories. , Environmental Science and Technology, DOI: 10.1021/es5049072, 2015.
Lu, W., and Wang, X.: Interaction patterns of major air pollutants in Hong Kong territory, Science of the Total Environment, 324, 247-259, 2004.
Marr, L. C., Moore, T. O., Klapmeyer, M. E., and Killar, M. B.: Comparison of NOx Fluxes Measured by Eddy Covariance to Emission Inventories and Land Use, Environmental Science & Technology, 47, 1800-1808, 10.1021/es303150y, 2013.
Mazzeo, N. A., Venegas, L. E., and Choren, H.: Analysis of NO, $NO_2$, $O_3$ and $NO_x$ concentrations measured at a green area of Buenos Aires City during wintertime, Atmospheric Environment, 39, 3055-3068, 2005.

Na, K., Moon, K.-C., and Kim, Y. P.: Source contribution to aromatic VOC concentration and ozone formation potential in the atmosphere of Seoul, Atmospheric Environment, 39, 5517-5524, 2005.
Newchurch, M., Ayoub, M., Oltmans, S., Johnson, B., and Schmidlin, F.: Vertical distribution of ozone at four sites in the United States, Journal of Geophysical Research: Atmospheres (1984–2012), 108, ACH 9-1-ACH 9-17, 2003.
Ohta, T., and Ohyama, T.: A set of rate constants for the reactions of OH radicals with aromatic hydrocarbons, Bulletin of the Chemical Society of Japan, 58, 3029-3030, 1985.
Pollack, I. B., Lerner, B. M., and Ryerson, T. B.: Evaluation of ultraviolet light-emitting diodes for detection of atmospheric $NO_2$ by photolysis-chemiluminescence, Journal of atmospheric chemistry, 65, 111-125, 2010.
Pudasainee, D., Sapkota, B., Bhatnagar, A., Kim, S.-H., and Seo, Y.-C.: Influence of weekdays, weekends and bandhas on surface ozone in Kathmandu valley, Atmospheric research, 95, 150-156, 2010.
Pugh, T. A., MacKenzie, A. R., Whyatt, J. D., and Hewitt, C. N.: Effectiveness of green infrastructure for improvement of air quality in urban street canyons, Environmental Science & Technology, 46, 7692-7699, 2012.
Rogers, T., Grimsrud, E., Herndon, S., Jayne, J., Kolb, C. E., Allwine, E., Westberg, H., Lamb, B., Zavala, M., and Molina, L.: On-road measurements of volatile organic compounds in the Mexico City metropolitan area using proton transfer reaction mass spectrometry, International Journal of Mass Spectrometry, 252, 26-37, 2006.
Schäfer, K., Heland, J., Lister, D. H., Wilson, C. W., Howes, R. J., Falk, R. S., Lindermeir, E., Birk, M., Wagner, G., and Haschberger, P.: Nonintrusive optical measurements of aircraft engine exhaust emissions and comparison with standard intrusive techniques, Applied Optics, 39, 441-455, 2000.
Schürmann, G., Schäfer, K., Jahn, C., Hoffmann, H., Bauerfeind, M., Fleuti, E., and Rappenglück, B.: The impact of NO, CO and VOC emissions on the air quality of Zurich airport, Atmospheric Environment, 41, 103-118, 2007.
Spicer, C., Holdren, M., Riggin, R., and Lyon, T.: Chemical composition and photochemical reactivity of exhaust from aircraft turbine engines, Annales Geophysicae, 1994, 944-955,
Stutz, J., Alicke, B., Ackermann, R., Geyer, A., White, A., and Williams, E.: Vertical profiles of NO3, N2O5, O3, and NOx in the nocturnal boundary layer: 1. Observations during the Texas Air Quality Study 2000, Journal of Geophysical Research: Atmospheres (1984–2012), 109, 2004.
Taipale, R., Ruuskanen, T., Rinne, J., Kajos, M., Hakola, H., Pohja, T., and Kulmala, M.: Technical Note: Quantitative long-term measurements of VOC concentrations by PTR-MS? measurement, calibration, and volume mixing ratio calculation methods, Atmospheric Chemistry and Physics Discussions, 8, 9435-9475, 2008.
Valach, A., Langford, B., Nemitz, E., MacKenzie, A., and Hewitt, C.: Concentrations of selected volatile organic compounds at kerbside and background sites in central London, Atmospheric Environment, 2014.
Velasco, E., Márquez, C., Bueno, E., Bernabé, R., Sánchez, A., Fentanes, O., Wöhrnschimmel, H., Cárdenas, B., Kamilla, A., and Wakamatsu, S.: Vertical distribution of ozone and VOCs in the low boundary layer of Mexico City, Atmospheric Chemistry and Physics, 8, 3061-3079, 2008.
Wang, S., Ackermann, R., Geyer, A., Doran, J. C., Shaw, W. J., Fast, J. D., Spicer, C. W., and Stutz, J.: Vertical variation of nocturnal NOx chemistry in the urban environment of Phoenix, Extended Abstracts, Fifth Conference on Atmospheric Chemistry in the 83rd AMS Annual Meeting, 2003,
Warneke, C., Van der Veen, C., Luxembourg, S., De Gouw, J., and Kok, A.: Measurements of benzene and toluene in ambient air using proton-transfer-reaction mass spectrometry: calibration, humidity dependence, and field intercomparison, International Journal of Mass Spectrometry, 207, 167-182, 2001.
Watson, J. G., Chow, J. C., and Fujita, E. M.: Review of volatile organic compound source apportionment by chemical mass balance, Atmospheric Environment, 35, 1567-1584, 2001.

Wesely, M., and Hicks, B.: A review of the current status of knowledge on dry deposition, Atmospheric Environment, 34, 2261-2282, 2000.

Table.1. Summary of meteorological and flight conditions during campaign.

| RF | Date | Time (local) | Mean Wind direction (°) | Mean Wind speed ($m\ s^{-1}$) | Mean True airspeed ($m\ s^{-1}$) | Mean Flight altitude a.g.l (m) |
|---|---|---|---|---|---|---|
| 1 | 24/6/13 | 15:30 – 18:20 | 285.9±17.1 | 13.6±3.3 | 81.1±3.9 | 603±28.9 |
| 2 | 26/6/13 | 16:00 – 18:00 | 287.5±17.0 | 3.8±1.0 | 70.7±3.4 | 349.8±15.1 |
| 3 | 27/6/13 | 9:40 – 12:15 | 277.6±20.9 | 4.2±1.4 | 69.6±2.7 | 354.1±11.1 |
| 4 | 27/6/13 | 14:20 – 17:50 | 275.1±24.5 | 6.6±1.6 | 72.6±5.4 | 343.1±31.7 |
| 5 | 3/7/13 | 10:40 – 13:00 | 280.7±11.0 | 6.3±1.3 | 71.9±4.0 | 366.1±7.2 |
| 6 | 4/7/13 | 15:20 – 16:55 | 240.7±11.3 | 7.5±1.4 | 72.5±4.5 | 365.1±18.3 |

Table.2. Summary of mixing ratios (ppbv) observed over inner London during campaign.

| | RF1 | RF2 | RF3 | RF4 | RF5 | RF6 |
|---|---|---|---|---|---|---|
| **Benzene** | | | | | | |
| **Mean** | 0.08 | 0.09 | 0.22 | 0.10 | 0.20 | 0.10 |
| **Median** | 0.07 | 0.09 | 0.15 | 0.09 | 0.19 | 0.10 |
| **SD** | 0.06 | 0.05 | 0.06 | 0.05 | 0.05 | 0.05 |
| **5$^{th}$ percentile** | 0.01 | 0.03 | 0.06 | 0.03 | 0.09 | 0.03 |
| **95$^{th}$ percentile** | 0.178 | 0.20 | 0.27 | 0.17 | 0.22 | 0.19 |
| **N** | 16500 | 13900 | 14100 | 2560 | 7620 | 11260 |
| **Toluene** | | | | | | |
| **Mean** | 0.17 | 0.12 | 0.28 | 0.15 | 0.28 | 0.12 |
| **Median** | 0.16 | 0.12 | 0.27 | 0.15 | 0.25 | 0.11 |
| **SD** | 0.07 | 0.08 | 0.11 | 0.07 | 0.07 | 0.09 |
| **5$^{th}$ percentile** | 0.08 | 0.06 | 0.05 | 0.05 | 0.12 | 0.01 |
| **95$^{th}$ percentile** | 4.34 | 0.26 | 0.39 | 0.32 | 0.38 | 0.28 |
| **N** | 16500 | 13900 | 14100 | 2560 | 7620 | 11260 |
| **NO** | | | | | | |
| **Mean** | 3.83 | 2.06 | 17.46 | 8.81 | 13.20 | 4.80 |
| **Median** | 3.46 | 2.44 | 16.19 | 7.76 | 12.43 | 3.41 |
| **SD** | 2.16 | 2.50 | 7.42 | 1.88 | 8.60 | 3.61 |
| **5$^{th}$ percentile** | 1.06 | 0.70 | 3.49 | 1.91 | 1.98 | 1.23 |
| **95$^{th}$ percentile** | 7.82 | 7.94 | 25.71 | 7.44 | 21.33 | 12.17 |
| **N** | 82500 | 69500 | 70500 | 12800 | 38100 | 56300 |
| **$NO_2$** | | | | | | |
| **Mean** | 15.19 | 11.99 | 22.95 | 18.64 | 21.02 | 12.17 |
| **Median** | 13.59 | 11.44 | 26.54 | 22.13 | 20.23 | 10.65 |
| **SD** | 6.10 | 8.29 | 13.17 | 7.89 | 6.38 | 7.31 |
| **5$^{th}$ percentile** | 7.56 | 7.91 | 11.45 | 10.21 | 6.03 | 3.65 |
| **95$^{th}$ percentile** | 26.49 | 31.90 | 52.13 | 35.08 | 25.97 | 19.60 |
| **N** | 82500 | 69500 | 70500 | 12800 | 38100 | 56300 |
| **$NO_x$** | | | | | | |
| **Mean** | 19.02 | 16.05 | 40.41 | 27.45 | 34.3 | 16.97 |
| **Median** | 17.49 | 17.91 | 36.02 | 26.78 | 32.40 | 15.95 |
| **SD** | 7.96 | 10.39 | 19.87 | 9.67 | 15.20 | 8.50 |
| **5$^{th}$ percentile** | 8.71 | 9.00 | 15.53 | 12.16 | 9.35 | 5.20 |
| **95$^{th}$ percentile** | 33.62 | 39.36 | 76.08 | 42.69 | 44.54 | 30.04 |
| **N** | 82500 | 69500 | 70500 | 12800 | 38100 | 56300 |

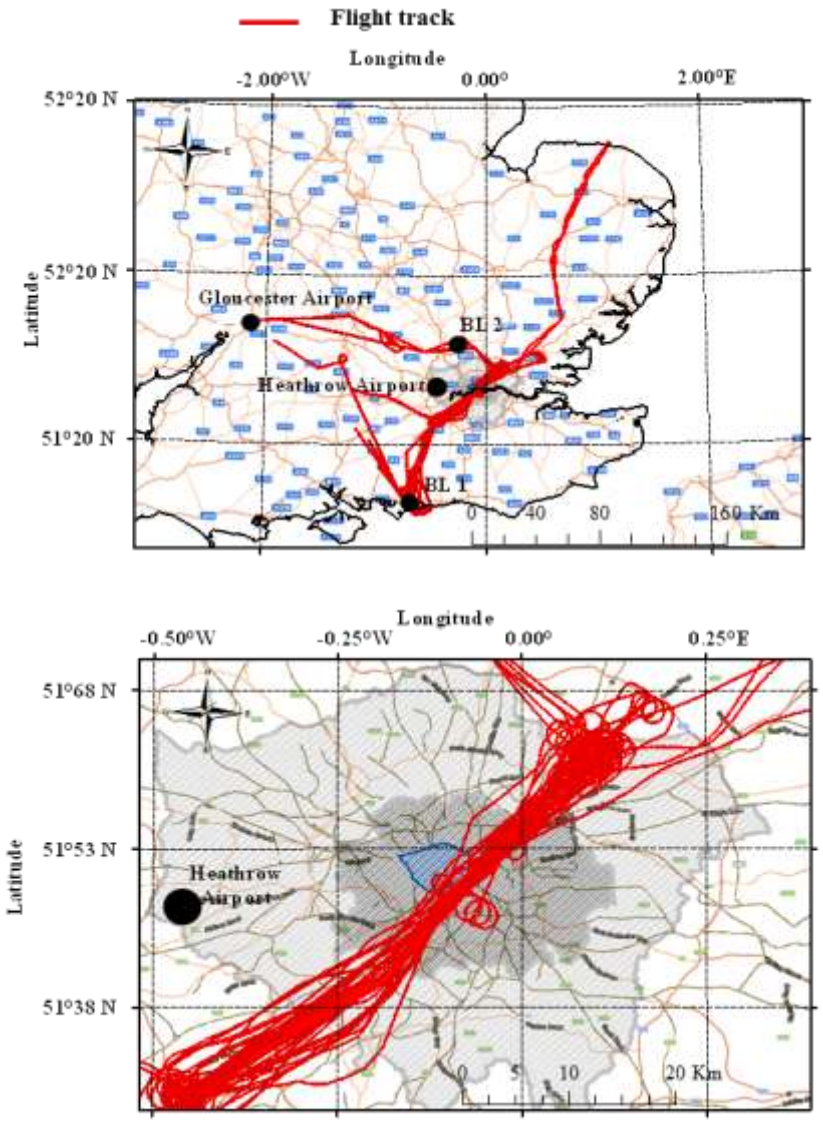


Figure 1a: top map showing all NERC Dornier-228 flights overlaid on UK transport map.

Figure 1b: bottom map showing total flight legs across Greater London. Grey area; Greater London boundary, black area; inner London boundary, blue area; London CCZ.

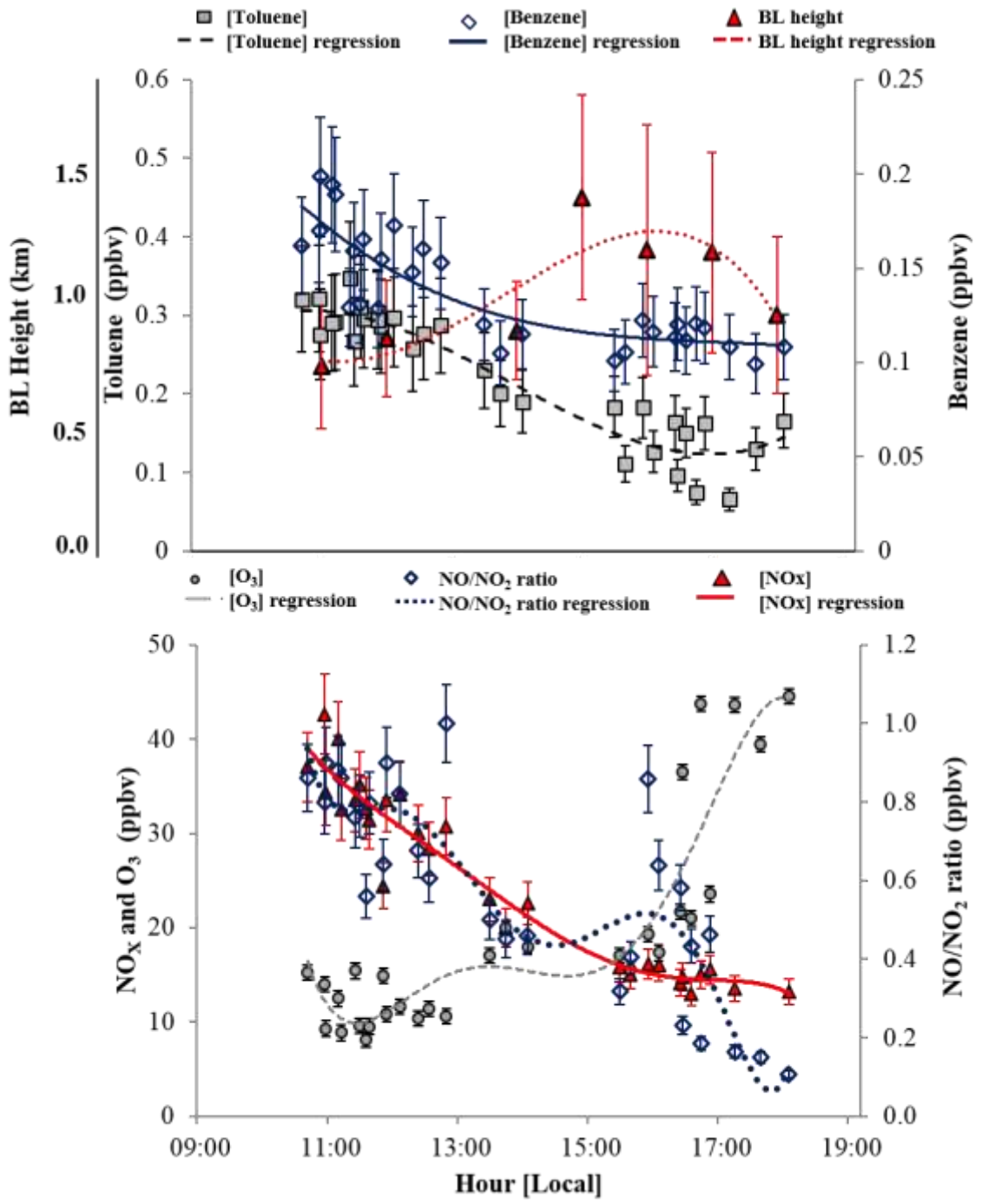


Figure 2. Top: time series of averaged benzene and toluene concentrations observed at 360±10 m a.g.l. during RF 2-6. Bottom: time series of averaged $NO/NO_2$ ratios and $O_3$, $NO_x$ concentrations during RF 2-6.

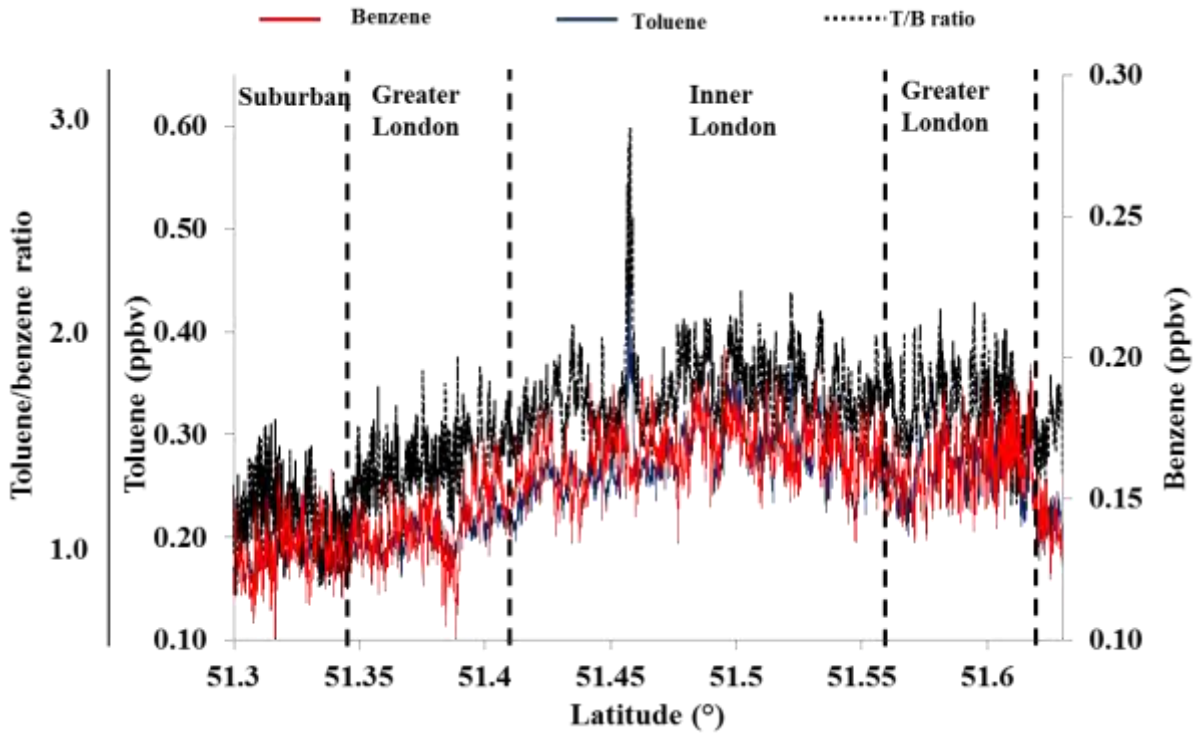


Figure 3. City cross section of 1km averaged benzene, toluene mixing ratios and T/B instantaneous ratios (ppbv ppbv$^{-1}$) at 360±10 m a.g.l. across Greater London during RF 5.

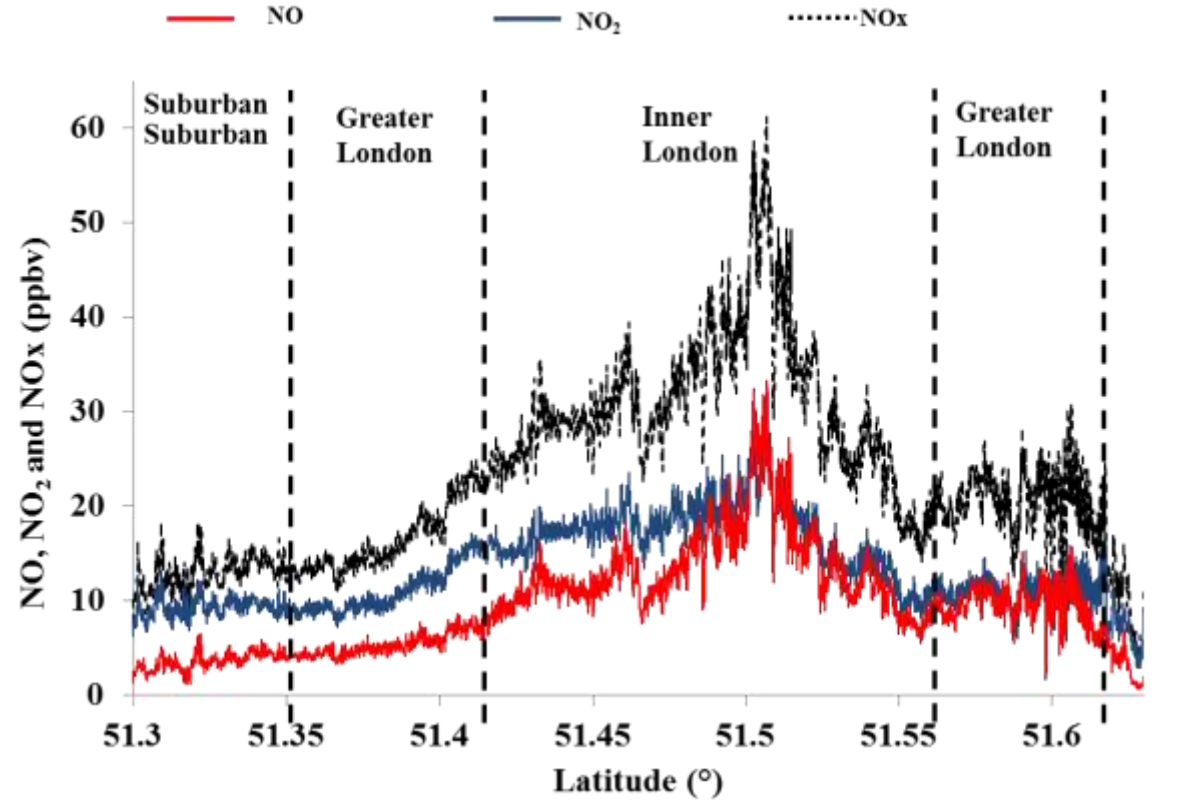


Figure 4. City cross section of 1km averaged NO $NO_2$ and $NO_x$ mixing ratios across Greater London at 360±10 m a.g.l. during RF 5.

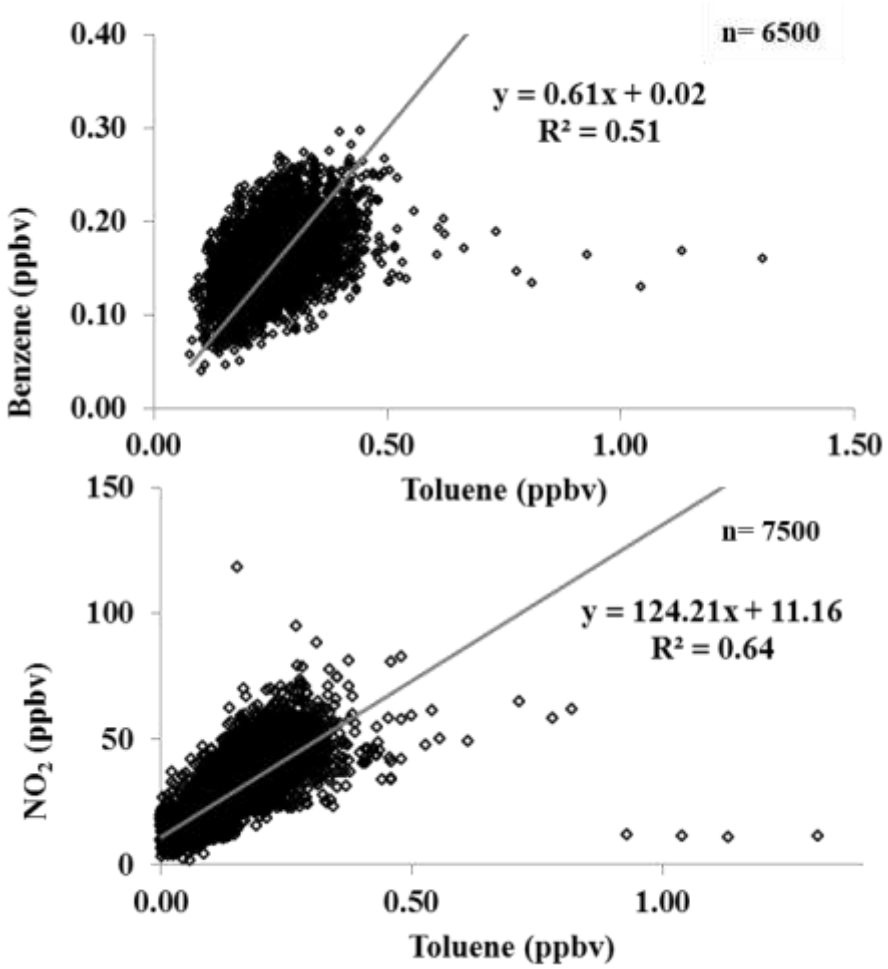


Figure.5. Top: linear regression analysis of benzene against toluene mixing ratios at 360±10 m a.g.l. during RF 5. Bottom: linear regression analysis of $NO_2$ against toluene mixing ratios at 360±10 m a.g.l. during RF 5.

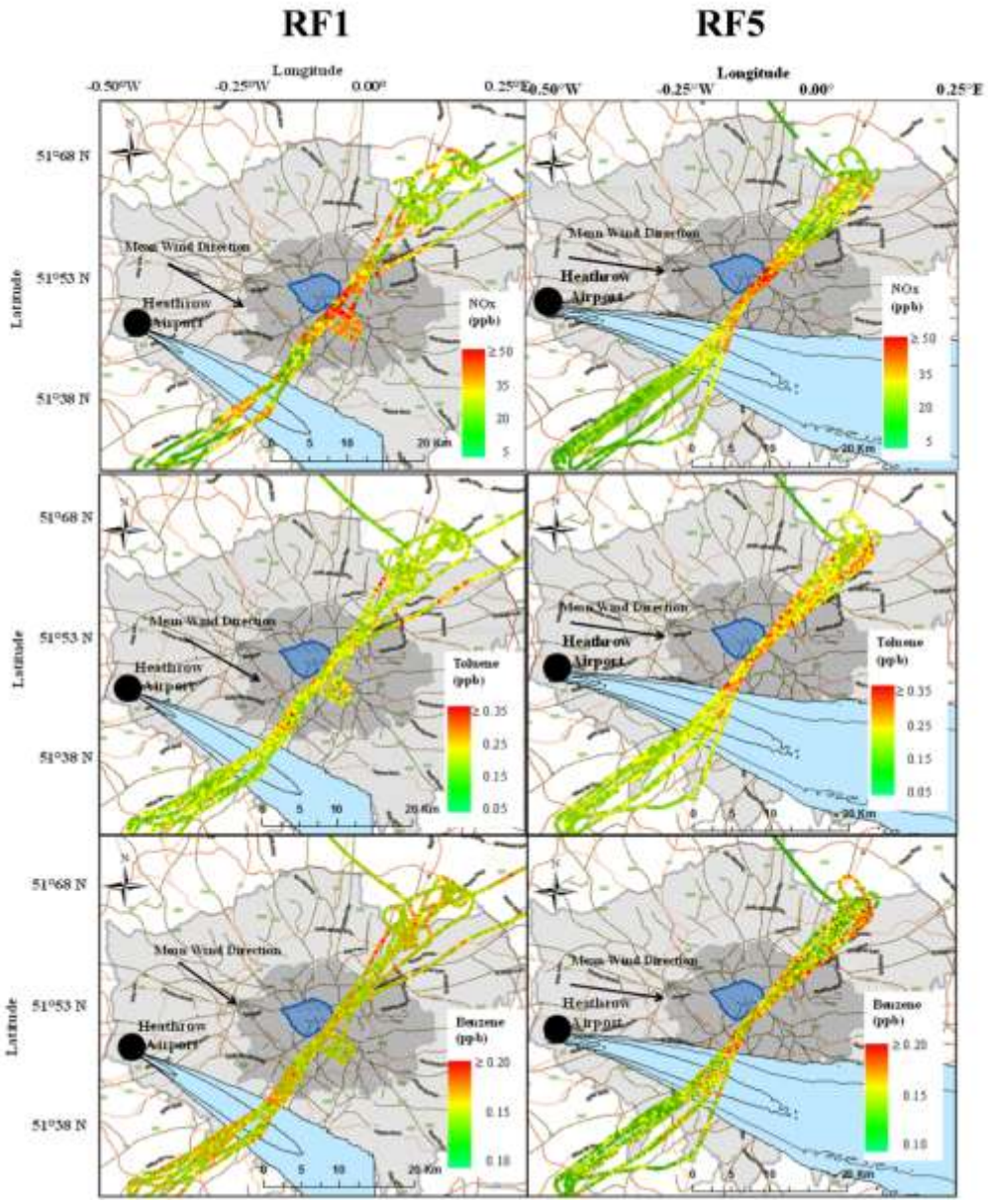


Figure 6. Top: NOx concentration data (7 metre resolved at 360±10 m a.g.l.) during RF1 (left) and RF5 (right) overlaid on UK transport map. Middle: Benzene concentration data (35 metre resolved at 360±10 m a.g.l.) during RF 1 (left) and RF5 (right) overlaid on UK transport map. Bottom: Toluene concentration data (35 metre resolved at 360±10 m a.g.l.) during RF1 (left) and RF5 (right) overlaid on UK transport map. Grey area; Greater London boundary, black area; inner London boundary, dark blue area; London CCZ, light blue area; 4 hour averaged HYSPLIT dispersion trajectory.

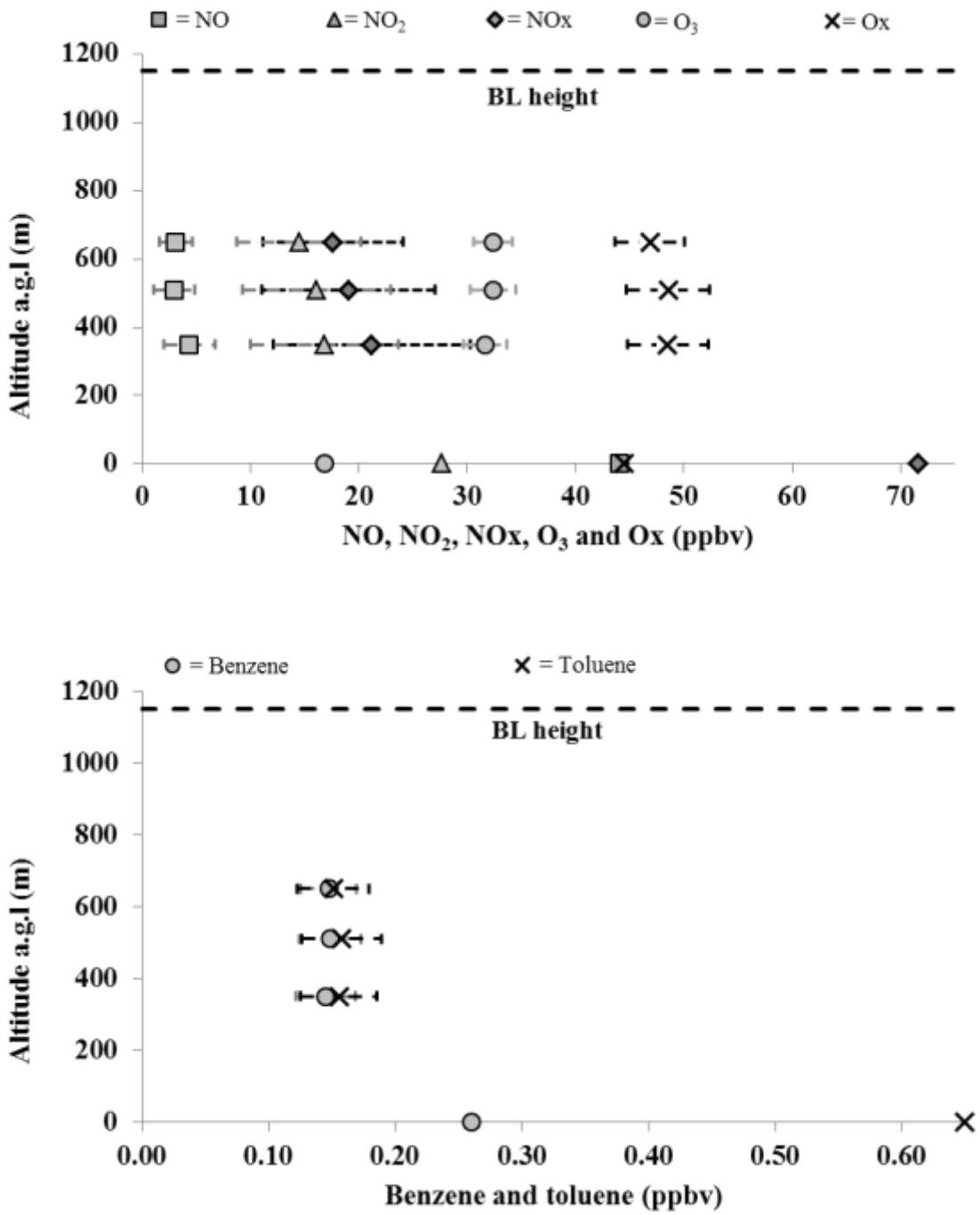


Figure 7. Average vertical profiles of $O_3$, NO, $NO_2$, $O_x$, benzene and toluene across London during RF1, 17:00 – 18:00 on the 24th of June 2013. X error bars represent standard deviation (1σ) of mixing ratios observed during each flight leg. Mixing ratio at ground level is hourly average from the LAQN Marylebone road air quality monitoring station.

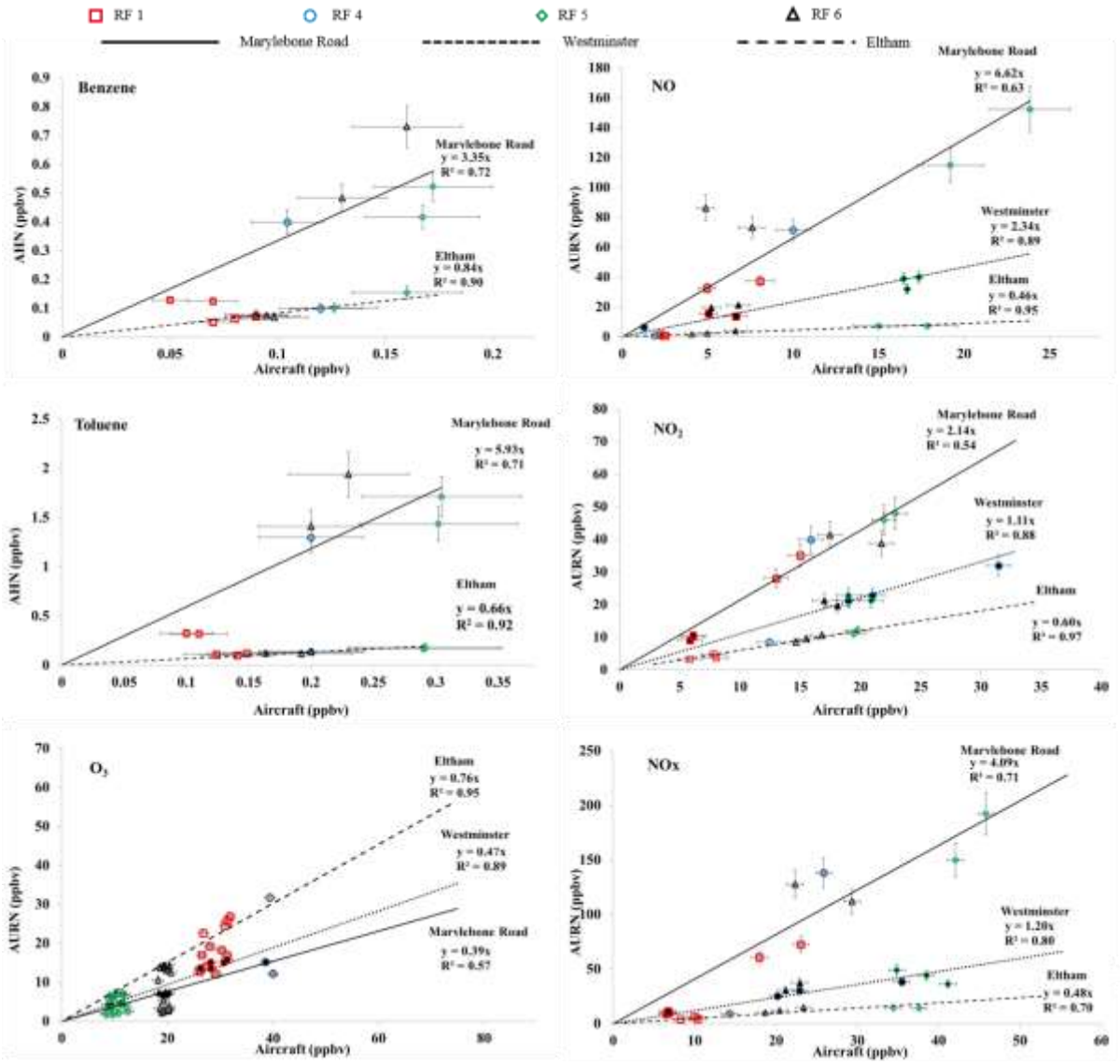


Figure 8. Linear regression analysis between airborne (at 360±10 m a.g.l.) and hourly ground measurements at Greenwich-Eltham (empty), Westminster-Horseferry road (black) and Marylebone Road (grey) from the LAQN monitoring network during RF1, 4, 5 and 6.